

Synthesis of Shaped, Reconfigurable, and Envelope Beam for Linear Array Using a Hybrid Whale Optimization Algorithm

Pengliang Yuan*

School of Cyberspace Security, Gansu University of Political Science and Law, Lanzhou 730070, China

ABSTRACT: Whale optimization algorithm (WOA) has been demonstrated to be a powerful strategy for various kinds of optimized problems. However, the direct use of WOA to tackle the shaped pattern synthesis can not reach the satisfactory result. To overcome this problem, a hybrid whale optimization algorithm (HWOA) is proposed in this paper, through integrating invasive weed optimization (IWO) and hyper chaotic system into the standard WOA to improve the population diversity and convergence speed. To demonstrate the performance of HWOA, various runs of tests are conducted for the most widely used benchmark functions. The statistical result shows that the proposed HWOA can attain a superior performance, in comparison with other state-of-the-art algorithms. To investigate the effectiveness and feasibility of the proposed HWOA in the linear array synthesis, the simulation experiments for synthesis of shaped, reconfigurable and envelope pattern in the main and side lobe are done, and the corresponding numerical results are provided. In the shaped beams synthesis, the specified peak side lobe level (PSLL) and maximal ripple are respectively -25 dB and 1 dB, and HWOA has a PSLL improvement of 0.2 dB and a ripple improvement of 0.27 dB. For the reconfigurable beams synthesis, the technique specification is the same as the shaped beams synthesis. The optimal PSLL reaches -25.57 dB, and the optimal ripple is 0.3873 dB. For the envelope synthesis, the main lobe region of line envelop lies in $\theta \in [85^\circ, 95^\circ]$, and the side lobe levels are decreased from -30 dB to -40 dB along a line. The maximal error of the optimal result is only 0.2 dB. In particular, a new form of fitness function to facilitate the envelope synthesis is also presented.

1. INTRODUCTION

The aim of shaped beam, reconfigurable beam and envelop synthesis are all to find the optimal amplitude and phase of the element excitation, which enable the synthesized pattern to approach the prescribed requirements as close as possible. The solution to the shaped beam synthesis and the reconfigurable beam synthesis includes the analytical methods [1–3] and numerical techniques [4–8]. Generally speaking, the analytical technique is only suitable for the specific problem. For the new problem, the origin analytical technique cannot always meet the requirement of practical problem, so that has to be redesigned. To overcome it, the numerical technique is introduced.

As a numerical technique, the evolutionary algorithm (EA) has been considered as an efficient candidate of solution to the array synthesis. For instance, the genetic algorithm [9–12] and simulated annealing [13–15] have been applied to synthesis of the shaped beam and reconfigurable beam.

Phase shifter plays a key role in the 5G technique, so there are many important studies based on phase shifter, such as [16, 17]. Since tuning the phase of excitation is easier than tuning the amplitude of excitation by a phase shifter in the practical feeding network, phase-only reconfigurable antenna array has been widely discussed in the past decades. In the meantime, some evolutionary algorithms have been applied to the synthesis of phase-only reconfigurable beam, such as genetic algorithm (GA) [18–20], particle swarm optimization (PSO) [20, 21], and differential evolution (DE) [22, 23]. With the deepening of

study, these EAs are also extended into synthesis of shaped beam in the side lobe region [20, 24–26].

In the recent years, most studies focus on using EAs to synthesize side lobe reduction and elements thinning for various types of antenna array. These EAs involve PSO [27], artificial bee colony algorithm [28], and WOA [29].

WOA algorithm, proposed by Mirjalili and Lewis in 2016 [30], is widely used to train the multi-layer perceptron of the most popular neural network method [31]. For specific use, many improved algorithms based on WOA were proposed, such as an adaptive WOA [32] with faster convergence speed and less parameter dependency, a new training algorithm [33], and an enhanced WOA with the improvement of the solution accuracy, reliability, and convergence speed [34]. To effectively get rid of a local optimum and obtain the high precision and quick convergence, Levy light trajectory was embedded into the WOA for global optimization [35]. Meanwhile, Levy light trajectory can also be used to solve feature selection [36], which is a major preprocessing step in eliminating the redundant, irrelevant variables within a dataset.

In our prior works, we have applied WOA in the synthesis of a nonuniform linear antenna array with a low PSLL [29], the synthesis of PSLL, null, and capacity in the presence of scatter WOA (used as an assistant) into salp swarm optimization to develop a hybrid algorithm for the synthesis of a conformal antenna array, which exhibits high convergence accuracy and faster convergence speed. The WOA is also used to diagnose the failures of antenna array [40] and comprehensively exam-

* Corresponding author: Pengliang Yuan (hamsir@126.com).

ine the design of 16-element linear array antenna (LAA) and time-modulated linear array (TMLA) [41].

For the synthesis of a concentric antenna array and an elliptical antenna array, an enhanced WOA algorithm hybridizes the solution initialization and crossover method [42], and a hybrid algorithm, based on the WOA and salp swarm optimization [43], is proposed, respectively.

Although much improvement has been made in WOA algorithm, the synthesis of a shaped, reconfigurable, and envelope beam by using WOA remains few. There are two main reasons:

1. the multiple reconfigurable beam synthesis mainly contains multiple constraints, which increase the difficulty of optimization.
2. EAs are not good at tackling this kind of problem, which is often solved by analytical method.

Additionally, WOA also has some evident disadvantages, such as the unbalanced problem between the exploitation and exploration, and falling into the local optima easily.

To overcome it, we propose a hybrid WOA algorithm integrated with IWO and Chen chaotic attractor. To the best of our knowledge, the research on hyper-chaotic system and evolutionary algorithm fusion has not been reported so far.

The remainder of this paper is organized as follows. Section 2 presents the layout of elements and formulation of pattern. In Section 3, the fitness function is provided for the synthesis of shaped, reconfigurable, and envelop pattern. Section 4 offers the description of related components of HWOA. Section 5 provides architecture of the proposed HWOA and test results for the test benchmark functions. Section 6 offers a variety of simulation experiments and the corresponding results. Section 7 provides a summary of the whole paper and the future studies.

2. PROBLEM FORMULATION

Consider a linear array with N elements, which are arranged in the right half of x -axis. The radiation pattern of the linear array can be formulated as

$$f(\theta) = \sum_{n=1}^N I_n e^{i[k(n-1)d \cos \theta + \phi_n]} \quad (1)$$

where I_n means the n th element excitation amplitude; $k = 2\pi/\lambda$, λ stands for the wavelength; d is the inter-element spacing; θ denotes the angle measured from the normal to the array; ϕ_n means the phase of the n th element excitation.

3. DESIGN OF THE FITNESS FUNCTION

3.1. The Fitness on Shaped Pattern Synthesis

The angle range of pattern is represented as Θ , to facilitate description and divided into two parts: Θ_m and Θ_s , i.e., $\Theta = \Theta_m \cup \Theta_s$. Here, subscripts m and s mean the main lobe and side lobe region in the angle range of pattern.

In the region of main lobe, the synthesized pattern is denoted as $f(\theta)$, and the error δ_m between the synthesized and desired patterns can be designed as

$$\delta_m(\theta \in \Theta_m) = \begin{cases} f(\theta) - B_u(\theta), & f(\theta) > B_u(\theta) \\ f(\theta) - B_d(\theta), & f(\theta) < B_d(\theta) \\ 0, & \text{otherwise.} \end{cases} \quad (2)$$

where B_u and B_d mean the upper and lower boundaries of the desired pattern, respectively. To facilitate calculation during optimization, the angle region θ should be sampled by the given number Q_m . The sampled θ can be expressed as $\theta_i, i = 1, \dots, Q_m$. Then, Eq. (2) will be rewritten as

$$\check{\delta}_m = \left(\sum_{i=1}^{Q_m} \delta_m(\theta_i)^2 / Q_m \right)^{1/2} = \left| Q_m^{1/2} \right| \|\delta_m\| \quad (3)$$

where $\|\cdot\|$ denotes the ℓ_2 -norm of a vector, and $\delta_m = \{\delta_m(\theta_i) | i = 1, \dots, Q_m\}$ is a vector.

In the region of side lobe, the error δ_s between the synthesized and desired patterns can be expressed as

$$\delta_s(\theta \in \Theta_s) = \begin{cases} f(\theta) - \text{PSLL}, & f(\theta) > \text{PSLL} \\ 0, & \text{otherwise.} \end{cases} \quad (4)$$

where PSLL stands for the peak of side lobe level of synthesized pattern. The angle region θ is sampled by the specified number Q_s . The sampled θ can be expressed as $\theta_j, j = 1, \dots, Q_s$. Similar to Eq. (3), Eq. 4 can be converted as

$$\check{\delta}_s = \left(\sum_{j=1}^{Q_s} \delta_s(\theta_j)^2 / Q_s \right)^{1/2} = \left| Q_s^{1/2} \right| \|\delta_s\| \quad (5)$$

where δ_s is a vector, $\delta_s = \{\delta_s(\theta_i) | i = 1, \dots, Q_s\}$.

In this synthesis problem, both constraints of main lobe and side lobe region need to be considered during optimization. Thereby the error $\check{\delta}_m$ and $\check{\delta}_s$ are aggregated into the fitness function. The fitness function can be formulated as

$$\text{fitness} = \alpha \check{\delta}_m + \beta \check{\delta}_s \quad (6)$$

where α and β are the control parameters for optimization; α is used to control the part of main lobe; and β is applied to control the part of side lobe. In the side lobe region, the aim of optimization is to obtain the optimal pattern, owning a lower PSLL than the desired PSLL. In the practical optimization, $\beta \check{\delta}_s$ of Eq. (6) can be replaced with the following

$$\beta \cdot \max\{\text{PSLL} - \text{PSLL}_d, 0\} \quad (7)$$

3.2. The Fitness on Reconfigurable Pattern Synthesis

In the synthesis of reconfigurable beams, the excitation amplitude together with varying phase of array will generate different shapes of patterns.

Suppose that the element number is N and that the number of reconfigurable beams is M . These beams have their own excitation phases, but they share a common excitation amplitude

$\{I_1, \dots, I_N\}$. Thus, the dimension of decision variables to be optimized will be $(M + 1)N$, which can be illustrated as

$$\left[\underbrace{I_1, \dots, I_N}_{\text{Common excitation}}, \underbrace{\phi_1^1, \dots, \phi_N^1}_{\text{Phase of the 1st beam}}, \dots, \underbrace{\phi_1^M, \dots, \phi_N^M}_{\text{Phase of the Mth beam}} \right] \quad (8)$$

The m th set of phase and the common excitation will generate the m th reconfigurable pattern. According to Eq. (1), the m th pattern can be expressed as

$$f_m(\theta) = \sum_{n=1}^N I_n \cdot e^{i[k(n-1)d \cos \theta + \phi_n^m]}, \quad m = 1, \dots, M. \quad (9)$$

where ϕ_n^m denotes the n th element phase of the m th reconfigurable pattern, and the meaning of the remaining parameters are the same as that of Eq. (1).

For the synthesis of reconfigurable pattern, the optimization problem can be formulated as

$$\min_{I_n^m, \phi_n^m} \text{fitness} \quad (10)$$

$$\text{s.t. } \{I_n^1 | n = 1, \dots, N\} = \dots = \{I_n^M | n = 1, \dots, N\} \quad (11)$$

$$\max(f(\theta)) \leq \text{PSLL}_d, \quad \theta \in \Theta_s \quad (12)$$

$$B_d \leq f(\theta) \leq B_u, \quad \theta \in \Theta_m \quad (13)$$

where I_n^m represents the excitation of the n th element generating the m th pattern; PSLL_d means the prescribed desired PSLL; B_d and B_u mean the lower and upper boundaries of the desired pattern, respectively. Eq. (12) and Eq. (13) represent the constraints of the side lobe and main lobe region, respectively.

When $M = 2$, the optimization problem (10) corresponds to a synthesis problem of two reconfigurable patterns. The fitness function of the first pattern is defined as

$$\text{fit}^{(1)} = \check{\delta}_m^{(1)} + \check{\delta}_s^{(1)} \quad (14)$$

where $\check{\delta}_m^{(1)}$ and $\check{\delta}_s^{(1)}$ are computed by Eq. (3) and Eq. (5), respectively. Similarly, the fitness of the second pattern can be given as follows

$$\text{fit}^{(2)} = \check{\delta}_m^{(2)} + \check{\delta}_s^{(2)} \quad (15)$$

The total fitness will be written as

$$\text{fitness} = \text{fit}^{(1)} + \text{fit}^{(2)} \quad (16)$$

For the synthesis of three reconfigurable beams, the total fitness is similar to Eq. (16).

3.3. The Fitness on the Envelop Pattern Synthesis

In the existing literature, the synthesis of envelop pattern often adopts Eq. (6) as the fitness of optimization. However, as far as HWOA is concerned, this fitness function does not work to synthesize the envelop pattern. Using Eq. (6) is difficult to attain a satisfactory envelope of beam. More specifically, all levels in the side lobe region will gather on a line under this circumstance. Through analysis, we find that this result is mainly caused by adopting the fitness Eq. (6), which cannot correctly

distinguish the peak and null at each lobe of the side lobe region.

To overcome it, we design a new fitness function, having an ability to identify the peak and null of each lobe. For the peak of pattern, the fitness can be defined as

$$\text{fit}_1 = \left| Q_u^{\frac{1}{2}} \right| \| \mathbf{E}(\boldsymbol{\theta}_u) - \mathbf{f}(\boldsymbol{\theta}_u) \|, \quad \boldsymbol{\theta}_u \in \Theta_s \quad (17)$$

where Q_u represents the total number of peaks for all lobes; \mathbf{E} means the desired envelop over $\boldsymbol{\theta}_u$; $\boldsymbol{\theta}_u$ represents a vector of locations corresponding to all peaks; $\mathbf{f}(\boldsymbol{\theta}_u)$ means the vector of synthesized pattern corresponding to the location vector $\boldsymbol{\theta}_u$.

For the null of pattern, the fitness can be defined as

$$\text{fit}_2 = \left| Q_v^{\frac{1}{2}} \right| \| (\mathbf{f}(\boldsymbol{\theta}_v) - \text{NULL}) \|, \quad \boldsymbol{\theta}_v \in \Theta_s \quad (18)$$

where Q_v represents the total number of nulls for all lobes; $\mathbf{f}(\boldsymbol{\theta}_v)$ denotes the vector of synthesized pattern corresponding to the location vector $\boldsymbol{\theta}_v$; $\boldsymbol{\theta}_v$ stands for the position vector of all nulls; NULL denotes a desired null level. Then, the total fitness can be written as

$$\text{fitness} = \text{fit}_1 + \text{fit}_2 \quad (19)$$

4. DESCRIPTION OF THE RELATED COMPONENTS OF HWOA

4.1. WOA

WOA is a heuristic evolutionary algorithm [30], which searches for the optimal solution by mimicking the hunting behavior of the humpback whale. Due to the simple structure and fewer tuning parameters than many of the evolutionary algorithms, WOA has been widely applied in various fields.

The mathematical model of WOA mainly contains three parts: encircling prey, spiral bubble-net feeding maneuver, and search for prey [30]. The role of encircling prey is to define a candidate search space to update the positions of target, further to search and obtain the optimum solution of optimization problem. This process can be represented as

$$\mathbf{x}(t+1) = \mathbf{x}^*(t) - A \cdot \mathbf{D} \quad (20)$$

where

$$\mathbf{D} = |C \cdot \mathbf{x}^*(t) - \mathbf{x}(t)| \quad (21)$$

where t denotes the iteration times; $\mathbf{x}^*(t)$ is the current optimal solution; $\mathbf{x}(t+1)$ is a candidate solution used in next iteration; $A = 2a\alpha - \alpha$ and $C = 2r$ are the control parameter, respectively, where α is linearly decreased from 2 to 0, and r is a random number from 0 to 1. The spiral bubble-net feeding maneuver has two ways to approach the optimal solution. One is shrinking encircling mechanism along the horizon direction, and the other is spiral updating mechanism along the vertical direction. The shrinking encircling mechanism is realized mainly by (20) and (21) by adjusting A with varying r and a . The spiral updating mechanism can be formulated as

$$\mathbf{x}(t+1) = \mathbf{D}' \cdot e^{bl} \cos(2\pi l) + \mathbf{x}(t) \quad (22)$$

TABLE 1. Description of test benchmark function.

Name	Function	V_{no}	Range	f_{min}
Rastrign	$F_1(x) = \sum_{i=1}^n [x_i^2 - 10 \cos(2\pi x_i) + 10]$	30	$[-5.12, 5.12]$	0
Ackley	$F_2(x) = -20 \exp(-0.2 \sqrt{\frac{1}{n} \sum_{i=1}^n x_i^2}) - \exp(\frac{1}{n} \sum_{i=1}^n \cos(2\pi x_i)) + 20 + e$	30	$[-32, 32]$	0
Griewank	$F_3(x) = \frac{1}{4000} \sum_{i=1}^n n x_i^2 - \prod_{i=1}^n n \cos(\frac{x_i}{\sqrt{i}}) + 1$	30	$[-600, 600]$	0
Penalized 1	$F_4(x) = \frac{\pi}{n} \{10 \sin(\pi y_1) + \sum_{i=1}^{n-1} (y_i - 1)^2 [1 + 10 \sin^2(\pi y_{i+1}) + (y_n - 1)^2] + \sum_{i=1}^n u(x_i, 10, 100, 4)\}$ $y_i = 1 + \frac{x_i + 1}{4}, u(x_i, a, k, m) = \begin{cases} k(x_i - a)^m, & x_i > a \\ 0, & -a < x_i < a \\ k(-x_i - a)^m, & x_i < -a \end{cases}$	30	$[-50, 50]$	0
Penalized 2	$F_5(x) = 0.1 \{ \sin^2(3\pi x) + \sum_{i=1}^n (x_i - 1)^2 [1 + \sin^2(3\pi x_i + 1)] + (x_n - 1)^2 [1 + \sin^2(2\pi x_n)] \} + \sum_{i=1}^n u(x_i, 5, 100, 4)$	30	$[-50, 50]$	0
Kowalik	$F_6(x) = \sum_{i=1}^{11} [a_i - \frac{x_1(b_i^2 + b_i x_2)}{b_i^2 + b_i x_3 + x_4}]^2$	4	$[-5, 5]$	0.003

where \mathbf{D} stands for the distance of the i th whale to prey and can be expressed as

$$\mathbf{D}' = |\mathbf{x}^*(t) - \mathbf{x}(t)| \quad (23)$$

When $|A| > 1$, the behaviour in search of solution is given by

$$\mathbf{x}(t + 1) = \mathbf{x}_{rand}(t) - A \cdot \mathbf{D} \quad (24)$$

where

$$\mathbf{D} = |C \cdot \mathbf{x}_{rand}(t) - \mathbf{x}(t)| \quad (25)$$

where $\mathbf{x}_{rand}(t)$ is a candidate solution produced by random generator(see [30] for more details).

4.2. IWO

IWO is a bio-inspired evolutionary algorithm imitating the reproduction behavior of weed [44], which mainly contains three parts: reproduction, spatial diffusion, and competitive exclusion.

In the phase of reproduction, each member of the population is allowed to produce seeds which depends on the lowest and highest fitness within the swarm. The seeds number is evaluated by the following equation

$$s = \left\lfloor \frac{fit_{max} - fit(x_i)}{fit_{max} - fit_{min}} (s_{max} - s_{min}) + s_{min} \right\rfloor \quad (26)$$

where s_{min} and s_{max} stand for the minimum and maximum of seed number; $fit(x_i)$ means the fitness of the i th weed; fit_{max} and fit_{min} are the minimum and maximum of fitness; $\lfloor \cdot \rfloor$ denotes the round down function.

The randomness and adaptability of IWO depend on the phase of spatial diffusion. After reproduction, the produced seeds will be distributed around the weeds with a normal distribution $N(0, \sigma_t^2)$, where σ_t means the standard deviation(std) at the current iteration and can be formulated as

$$\sigma_t = \sigma_{final} + \left(\frac{t_{max} - t}{t_{max}} \right)^w (\sigma_{initial} - \sigma_{final}) \quad (27)$$

where $\sigma_{initial}$ and σ_{final} are the initial value and the final value of std; t_{max} and t denote the maximum and current of iteration;

and w is a nonlinear regulatory factor. It indicates that in the beginning stage of evolution, the seeds will be placed in a space which is far away from the weeds. With the increasing of iteration, the distance between the seeds and the corresponding weeds will be decreased gradually, and the seeds will be placed near the weeds.

In the phase of competitive exclusion, the individuals with the worse fitness will be excluded from the whole population, in order to improve the quality of population and the efficiency of IWO. when the number of individuals exceeds P_{max} , the above operation will be made (see [44] for more details).

4.3. Chen Chaotic Attractor

Chen chaotic attractor is a hyper chaotic system [45], with more than one positive Lyapunov exponent and more complex dynamical characteristic than chaos, which can be expressed as follows

$$\begin{cases} \dot{x} = a(y - x) \\ \dot{y} = (c - a)x - xz + cy \\ \dot{z} = xy - bz \end{cases} \quad (28)$$

where $a, b, c,$ and d are constants. Only if $a = 36, b = 3, c = 28, d = -16$, the Chen chaotic attractor will enter the chaotic state. In this chaotic system, there are three Lyapunov exponents, including two non-positive Lyapunov exponents, and the corresponding figure is shown in Fig. 1.

5. THE PROPOSED ALGORITHM

5.1. Description of the Proposed Algorithm HWOA

In standard WOA, the capability of global search is achieved by a blind operator which is unrelated to the fitness of current solution. The existing literature has found that choosing a different selection mechanism helps EAs to improve the exploration ability [36], which inspires us to develop a new hybrid algorithm. To adapt the characteristic of array synthesis, the proposed algorithm uses IWO as the local search to replace Eq. (24), which has an advantage that the hybrid algorithm does not need to

tackle the problem of incompatibility between IWO and WOA. This is because the standard WOA evolves by element of individual, which is the same as IWO.

To enhance the diversity of candidate solution and achieve the aim of optimization efficiently, the best solution of each run will be further diffused by taking advantage of the chaotic mechanism, so that the algorithm can provide more chance for the weak solution.

In the existing literature, it has been demonstrated that the chaotic strategy can bring more stochastic property for the population [46]. Thus, we exploit the Chen chaotic attractor to diffuse the initial population in the beginning of HWOA, in order to achieve a better diversity and distribution. It has to address an issue that the dimension of population may not be the integer times of three inputs of this chaotic system. To circumvent it, we take a strategy that the rest of individual elements will be kept unchanged, namely, not enter the chaotic transform. The process of proposed HWOA algorithm is stated in Algorithm 1.

Algorithm 1 HWOA

Require:

- 0: $t = 0, iter_{max}$;
- 0: randomly generated N initial population X_i , then disturb the population using Eq. (28).

Ensure: x^* =the best search agent

- 1: **while** $t < iter_{max}$ **do**
 - 2: Initialize the parameters;
 - 3: **for** $i=1$ to N **do**
 - 4: Calculate the fitness of population;
 - 5: Update the best fitness and agent;
 - 6: Update a, A, C, l and p ;
 - 7: **if** $1(|A| < +1)$ **then**
 - 8: Update the position of the current solution by Eq. ((20)) and Eq. ((21));
 - 9: **else if** $1(|A| > +1)$ **then**
 - 10: Select a random search agent x_{rand} ;
 - 11: Update the position of the current search agent by IWO;
 - 12: **end if**
 - 13: Update the position of the current search by the Eq. ((22)) and Eq. ((23));
 - 14: **end for**
 - 15: Check if any solution goes beyond the search space and amend it;
 - Calculate the fitness of each solution;
 - Update x^* if there is a better solution;
 - $t = t + 1$.
 - 16: **end while**
-

5.2. Application of HWOA to Mathematical Functions

Generally, the number of object function evaluations under the given accuracy can be regarded as a good reference in the efficiency of an evolutionary algorithm. To illustrate the performance of the proposed approach, test is performed for the most widely used benchmark functions. These benchmark functions involve the multi-modal (F1–F5) and fixed-dimension func-

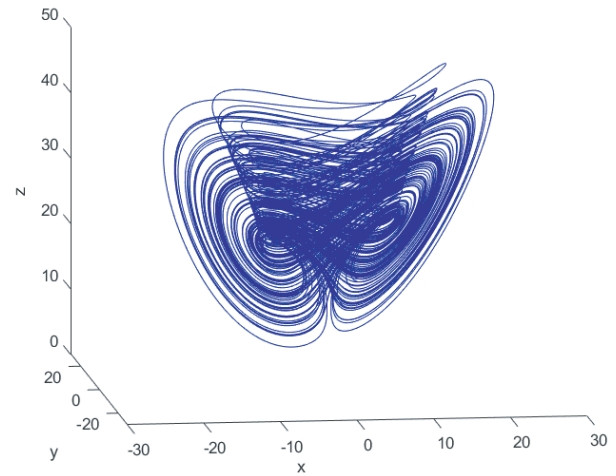


FIGURE 1. 3D figure of Chen chaotic attractor.

tions (F6), and the corresponding descriptions are listed in Table 1 in detail. It needs to note that the difference between the multi-modal and fixed-dimension functions is that the multi-modal function has capability of defining the desired number of optimization variables, but the fixed-dimension function cannot tune the desired number of optimization variables caused by the mathematical formulation. Moreover, the fixed-dimension function can provide different search spaces, and the multi-modal function has many of local optima whose number exponentially increases with the problem size. Thus, this kind of test benchmark function is helpful to evaluate the exploration capability of an algorithm.

In this test, the number of initial population is set as 30, and the iteration is assigned as 500. For each test benchmark function, the proposed algorithm HWOA is performed for 30 runs, which are based on the random generated initial population.

After multiple runs of tests, the statistic results are obtained, and the corresponding figures are given. The simulation results on average (Ave) and standard deviation (Std) are shown in Table 2. The corresponding convergence curves are depicted in Fig. 2, and the typical 2D plots of the cost functions and search history are provided in Fig. 3 and Fig. 4.

From Fig. 2, it can be seen that the obtained optimum of HWOA is better than the other comparable algorithms for all test benchmark functions. Table 2 indicates that the proposed algorithm HWOA has a good exploration capability, obtains a better fitness, and is the most efficient algorithm for the test benchmark functions.

6. SIMULATION RESULTS

To demonstrate the effectiveness and feasibility of the proposed HWOA in linear array synthesis, we provide several numerical examples, involving the shaped pattern synthesis for the main lobe region, reconfigurable pattern synthesis and envelope pattern synthesis for the side lobe region. The population size of HWOA is set as 40 in all examples. It needs to be pointed out that the dynamic range ratio (DRR) is defined as $DRR = \max(I_n) / \min(I_n)$.

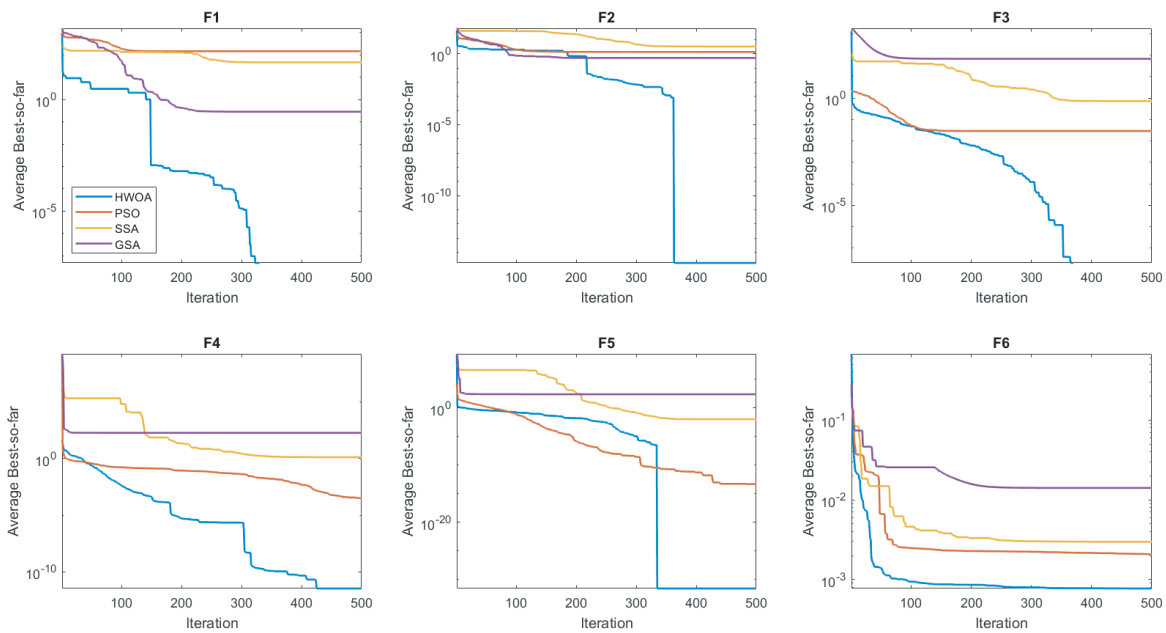


FIGURE 2. Comparison of convergence curves between HWOA and the other algorithms for the test benchmark function.

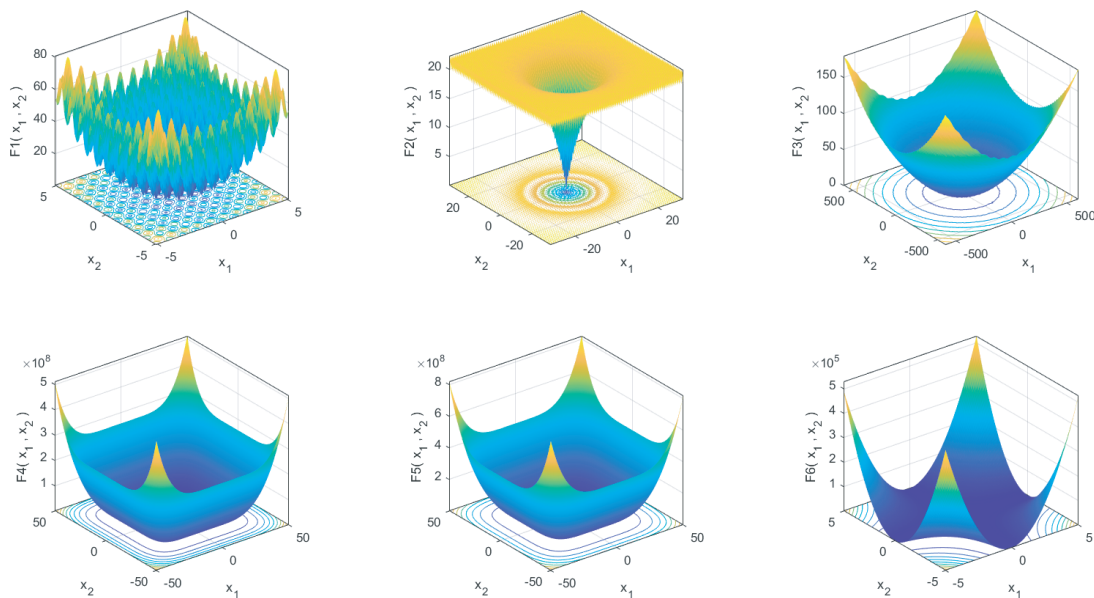


FIGURE 3. Typical 2D representations of test benchmark function.

6.1. Synthesis of Shaped Pattern

Considering a 17-element uniform isotropic source linear array, the excitation amplitude and phase are simultaneously optimized to enable the synthesized pattern to approach the desired shaped pattern as close as possible. In this case, we deal with two kinds of beams, including flat-top beam and cosecant beam. The related parameters of the desired shaped pattern are assigned as follows: the beam width is assigned as 40° ; the ripple should be less than 1 dB; and the PSLL should be less than -25 dB. The width of transition region between the main lobe

region and side lobe region should be constrained in 10° . The lower and upper boundaries of excitation amplitude should lie in $[0.01, 1]$.

To exhibit the superiority of HWOA, there are two widely used evolutionary algorithms (PSO and GA) introduced to make comparison. The parameters of PSO are assigned as follows: the population size is 40, the inertia weight factor $w = 0.4$, the acceleration constants $c_1 = c_2 = 2.0$, the maximum velocity $V_{\max} = 1.0$. The parameters of GA are set as: population size is 40; the crossover and mutation probabilities

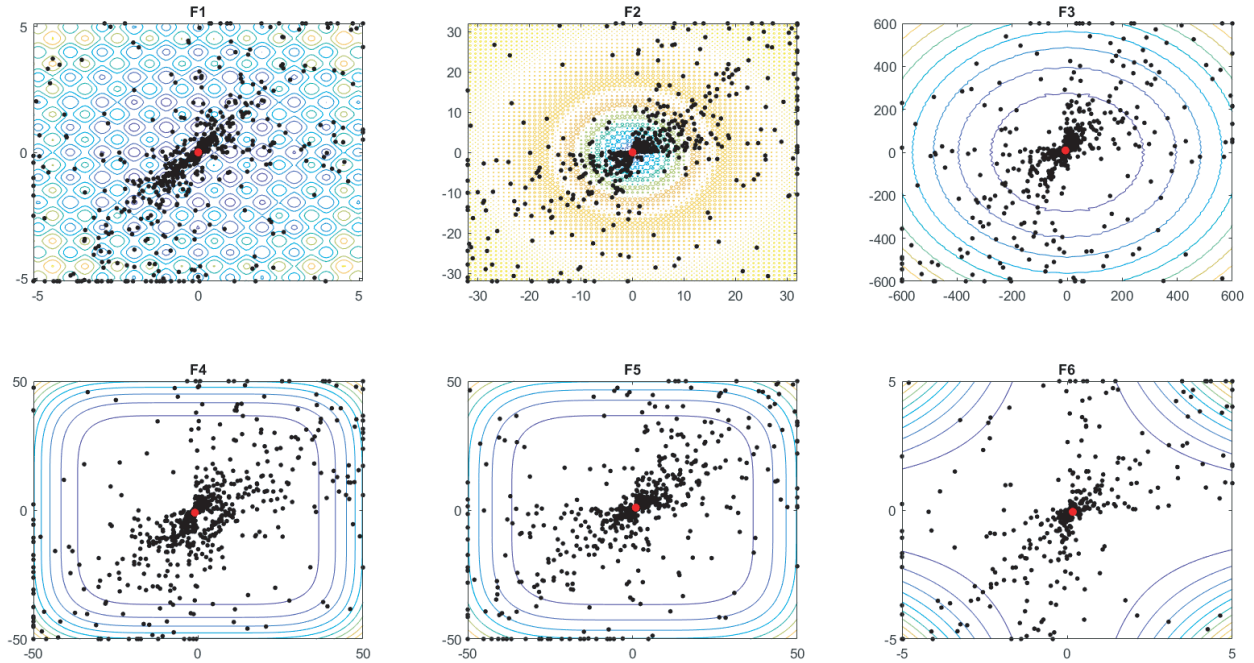


FIGURE 4. Search history of test benchmark function(red dot represents the final optimum of test benchmark function).

TABLE 2. Numerical results for test on benchmark function.

Item	Algorithm	F1	F2	F3	F4	F5	F6
Ave	GSA	9.44E-02	1.69E-01	2.27E+01	5.92E+01	8.33E+01	7.04E-03
	PSO	7.21E+01	6.70E-01	1.47E-02	1.46E-04	2.43E-14	1.04E-03
	SSA	1.53E+01	1.07E+00	2.44E-01	4.23E-01	3.66E-03	9.93E-04
	HWOA	0.00E+00	8.88E-16	0.00E+00	1.75E-12	1.35E-32	3.86E-04
Std	GSA	6.71E-02	1.18E-01	4.35E+00	7.81E+01	1.15E+02	2.35E-03
	PSO	5.47E+00	6.70E-01	1.47E-02	2.95E-06	3.11E-15	5.58E-04
	SSA	5.99E+00	1.52E+00	1.55E-01	4.50E-01	5.18E-03	1.86E-04
	HWOA	0.00E+00	0.00E+00	0.00E+00	6.19E-13	0.00E+00	5.90E-05

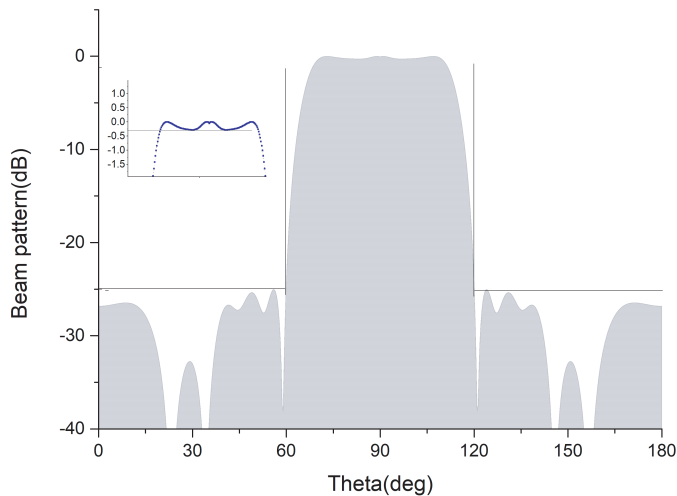


FIGURE 5. Synthesized flat-top pattern.

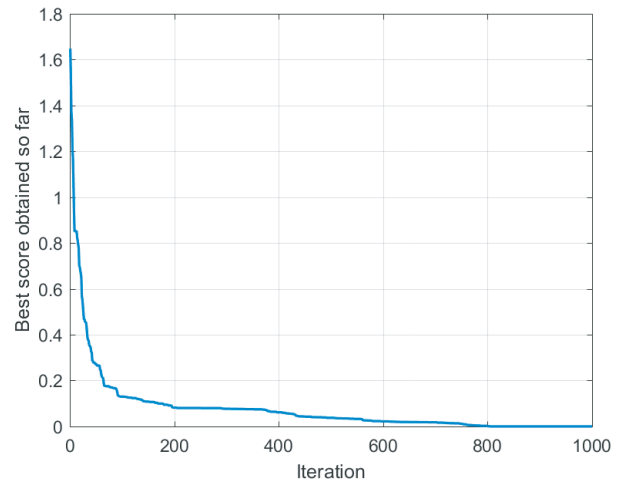


FIGURE 6. Convergence curve of synthesized flat-top pattern.

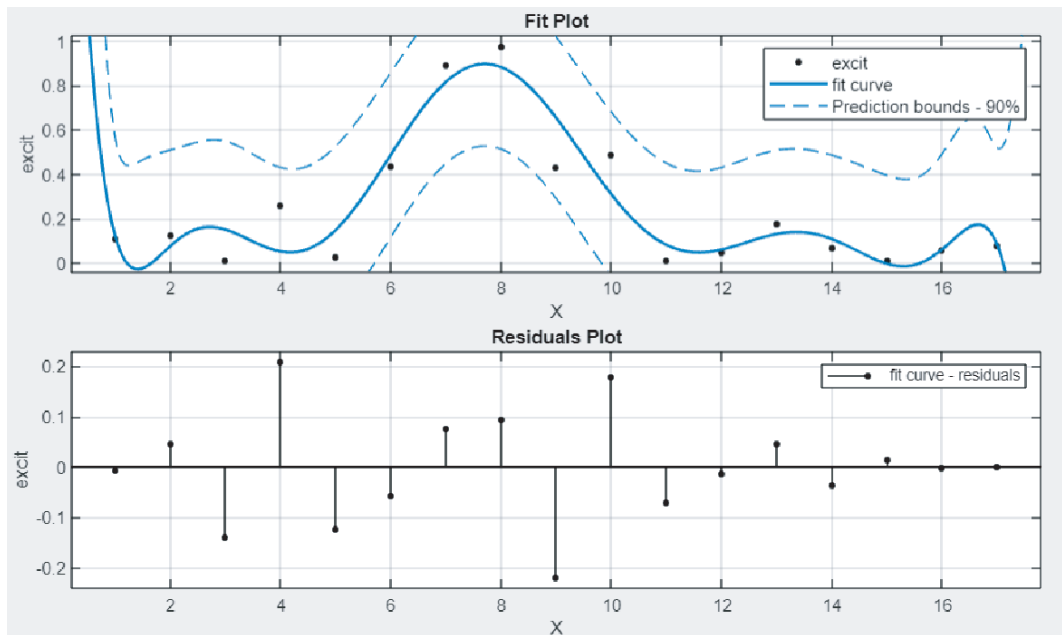


FIGURE 7. Excitation amplitude of synthesized flat-top pattern (X means the index of elements,the same below).

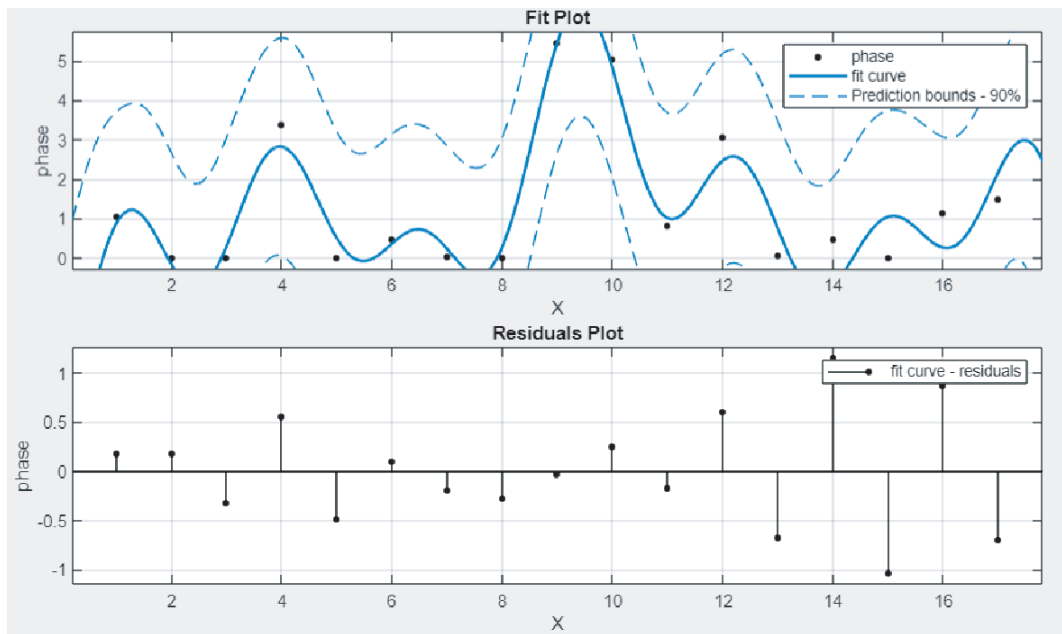


FIGURE 8. Excitation phase of synthesized flat-top pattern.

are 0.9 and 0.01; the selection parameter is 0.0005. To make fair comparison, the iteration numbers of PSO and GA are consistent with HWOA.

6.1.1. Flat-Top Pattern

The requirement of the desired pattern is just as the above description. After multiple runs of optimization, the proposed HWOA achieves the optimal synthesized pattern, as shown in Fig. 5. The convergence curve during the optimization is plot-

ted in Fig. 6, and the amplitude and phase of the excitation are depicted in Fig. 7 and Fig. 8. To see the trend of excitation clearly, the optimal excitation is fitted by the usual fit function. We also use the state-of-the-art algorithms of PSO and GA to achieve this synthesis, and their results are compared with HWOA. The comparison results are given in Table 3.

From Fig. 5 and Table 3, we can see that the synthesized pattern meets the requirements of the desired shaped pattern. More specifically, the ripple in the main lobe region of the synthesized pattern is measured at 0.2812 dB, which is far less than the

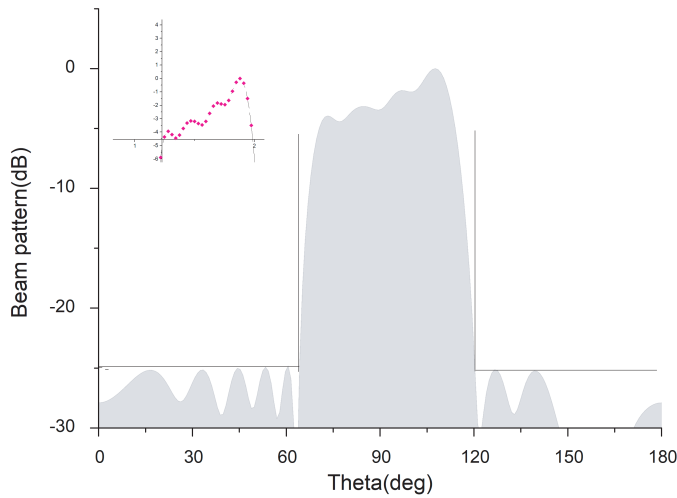


FIGURE 9. Synthesized cosecant pattern.

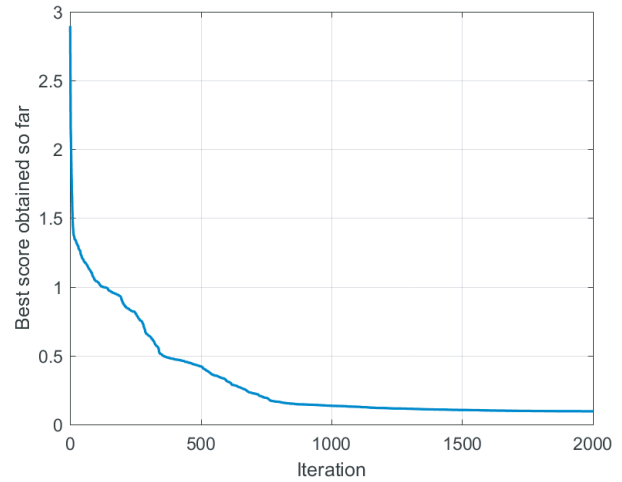


FIGURE 10. Convergence curve of synthesized cosecant pattern.

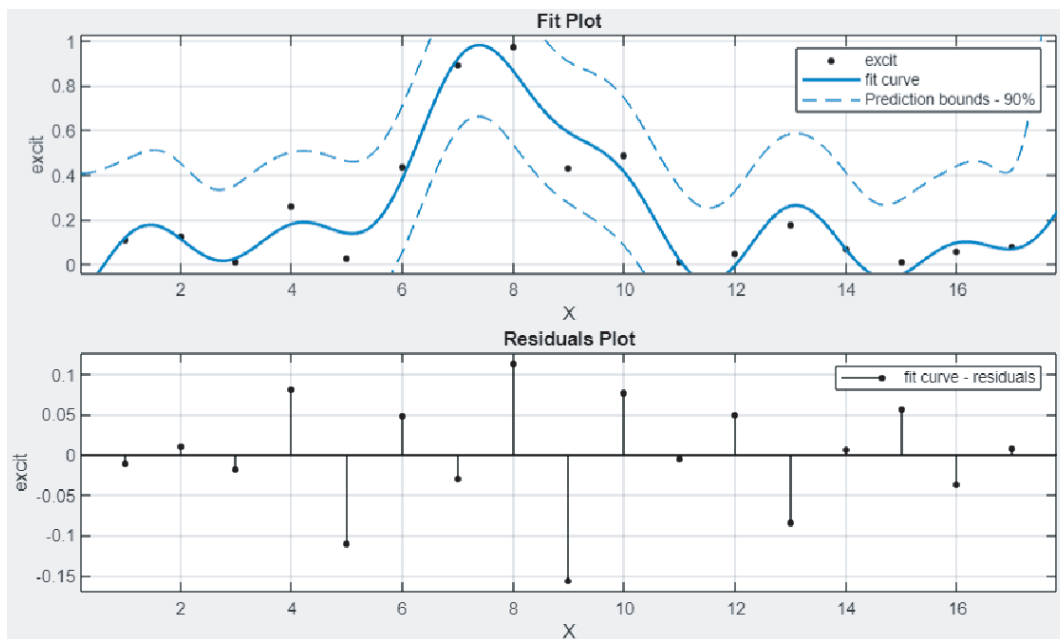


FIGURE 11. Excitation amplitude of synthesized cosecant pattern.

TABLE 3. Performance comparison between flat-top and cosecant pattern.

Beam	Item	GA	PSO	HWOA
Flat-top	Ripple(dB)	0.4695	0.4519	0.2812
	PSLL(dB)	-24.41	-25	-25.02
Cosecant	Ripple(dB)	1.0982	0.9545	0.5801
	PSLL(dB)	-25.17	-24.67	-25.02

prescribed 1 dB. The PSLL is measured at -25.02 dB, which also accomplishes the desired goal despite a marginal improvement. In contrast with GA and PSO, HWOA can obtain the best PSLL in the side lobe region and the best ripple in the main lobe region among them. The directivity and DRR are 0.0839 and

97.65. In summary, the proposed algorithm HWOA exhibits a better performance in this example.

6.1.2. Cosecant Pattern

The requirements of desired beam in this example are given at the beginning of Section 6.1.

Through multiple runs of optimization, the optimal results are obtained, and the corresponding figures are provided. The optimal cosecant pattern obtained by HWOA is plotted in Fig. 9, where the ripple is measured at 0.2812 dB, and the corresponding PSLL is -25.02 dB. They all achieve the prescribed goals. The convergence curve over the iteration is given in Fig. 10. The optimal amplitude and phase of excitation are given in Fig. 11 and Fig. 12. We make further performance

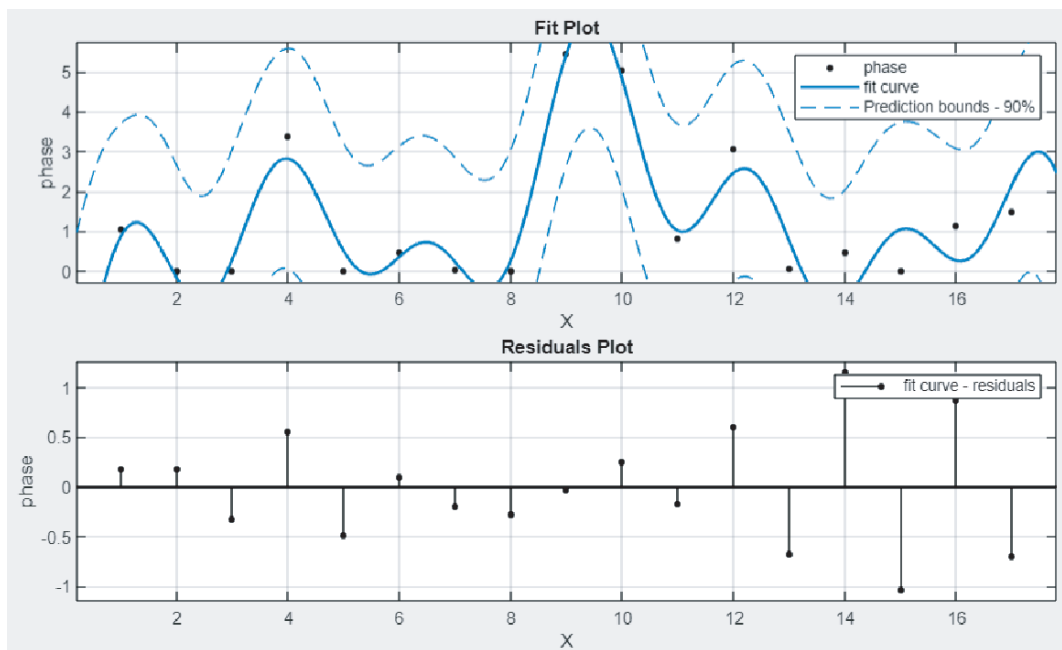


FIGURE 12. Excitation phase of synthesized cosecant pattern.

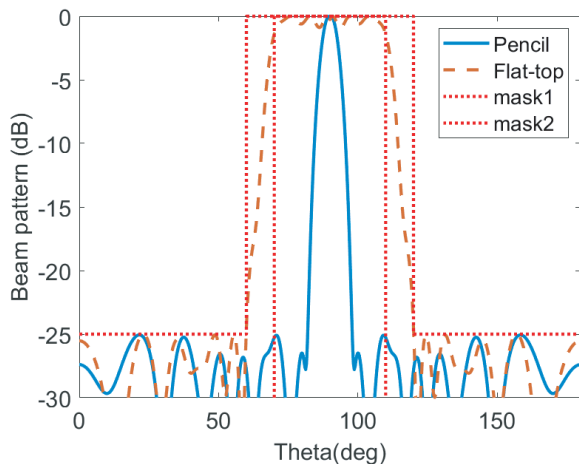


FIGURE 13. Synthesized pencil and flat-top pattern.

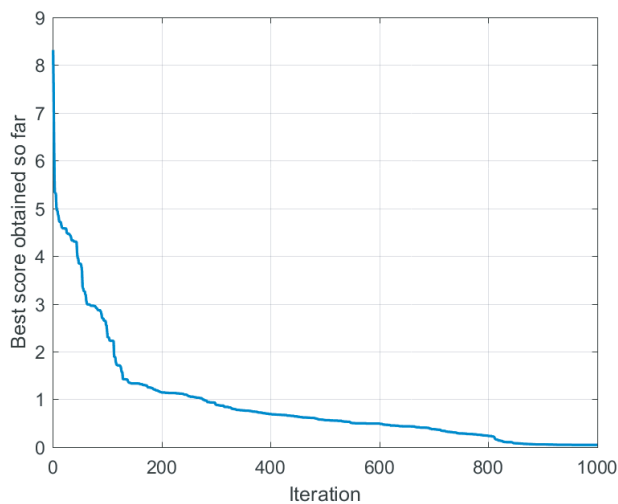


FIGURE 14. Convergence curve of synthesized pencil and flat-top pattern.

comparison among HWOA, GA, and PSO, and the corresponding results are listed in Table 3. From Table 3, it can be seen that the PSLL and the ripple obtained by HWOA all achieve the goals, while GA only meets the desired PSLL. In Fig. 11 and Fig. 12, we can see that the amplitude of excitation presents a relatively regular curve like a sin function, and the phase of excitation seems like a saddle. The directivity and DRR are 0.4443 and 10.00.

6.2. Synthesis of Reconfigurable Pattern

6.2.1. Pencil Pattern vs Flat-Top Pattern

In this example, two reconfigurable beams involving the pencil beam and flat-top beam are synthesized by using HWOA. The

requirements on the desired patterns are as follows: in the desired pencil pattern, the beam width should be expected to be located in $[80^\circ, 100^\circ]$, and the desired PSLL should be less than -25 dB. The requirement of the desired flat-top pattern is the same as that of Section 6.1.

Through various runs of optimization, the obtained optimal beams and convergence curve are shown in Fig. 13 and Fig. 14. The corresponding common excitation amplitude and phase are depicted in Fig. 15 and Fig. 16. Through the measurement of the obtained optimal beams, the maximal ripple and the PSLL of the flat-top pattern reach 0.5228 dB and -25.49 dB, respectively. In the pencil pattern, HWOA obtains a PSLL of -25.02 dB and a beam width that is not greater than 20° . Both of the synthesized patterns achieve the prescribed goals. The

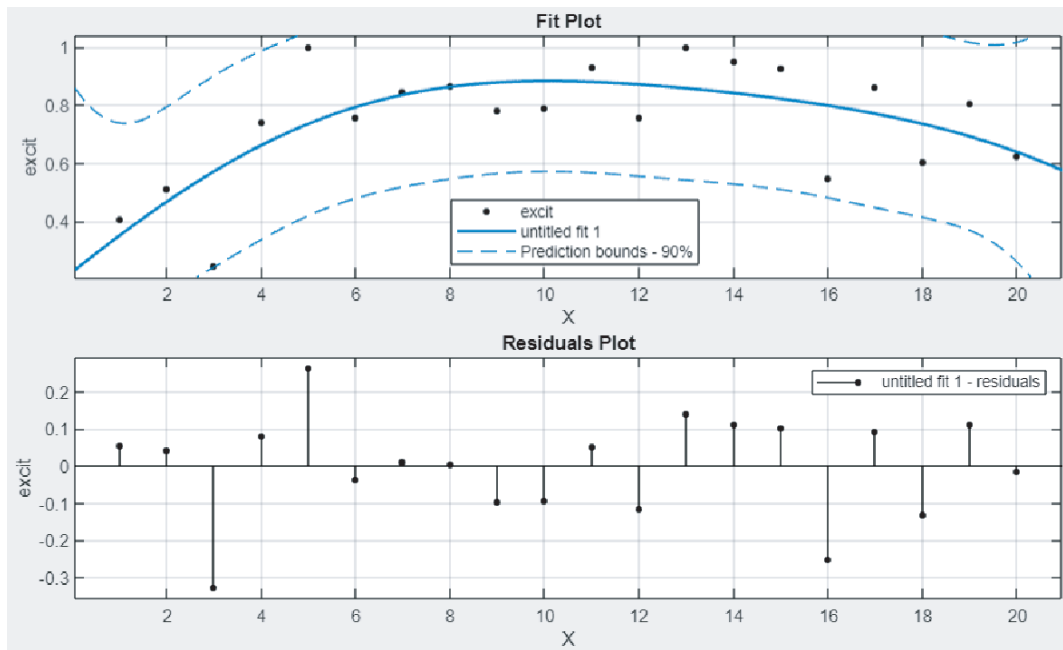


FIGURE 15. Common excitations of synthesized pencil and flat-top pattern.

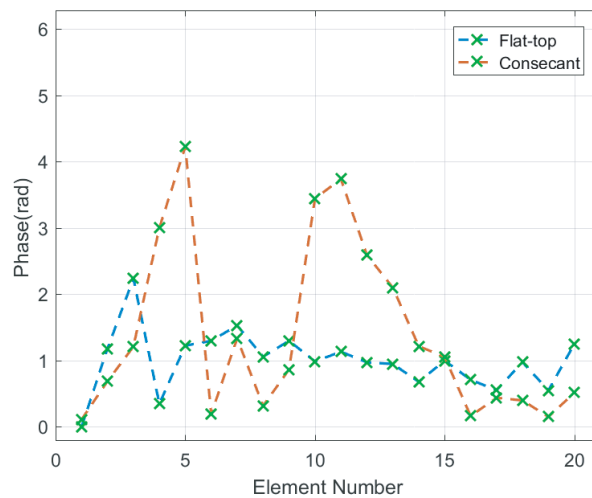


FIGURE 16. Excitation phase of synthesized pencil and flat-top pattern.

directivities of pencil and flat-top are 0.5157 and 0.0948, and DRR is 4.09.

6.2.2. Cosecant Pattern vs Flat-Top Pattern

The requirements of the desired patterns are the same as in Section 6.1. Through the optimization, the optimal results are obtained by using HWOA.

The synthesized patterns and convergence curve are shown in Fig. 17 and Fig. 18. The optimal excitation amplitude and phase are plotted in Fig. 19 and Fig. 20. The maximal ripples of the flat-top pattern and cosecant pattern reach 0.3873 dB and 0.4261 dB, respectively. Both PSLLs are less than the prescribed PSLL of -25 dB. It is evident that the ripples and

PSLLs of both patterns accomplish the prescribed goals. The directivities of the flat-top beam and cosecant beam are 0.2871 and 0.4720, and DRR is 100.

6.2.3. Pencil Pattern vs Cosecant Pattern

The requirements of the desired pencil pattern and cosecant pattern are the same as in Section 6.1. The optimal pattern and convergence curve obtained by HWOA are shown in Fig. 21 and Fig. 22. The corresponding excitation amplitude and phase are depicted in Fig. 23 and Fig. 24. The synthesized pencil pattern has a PSLL of -25.05 dB and a beam width of 79.03° . The synthesized cosecant pattern has a PSLL of -25.36 dB and a maximal ripple of 0.8354 dB. It can be seen that the results

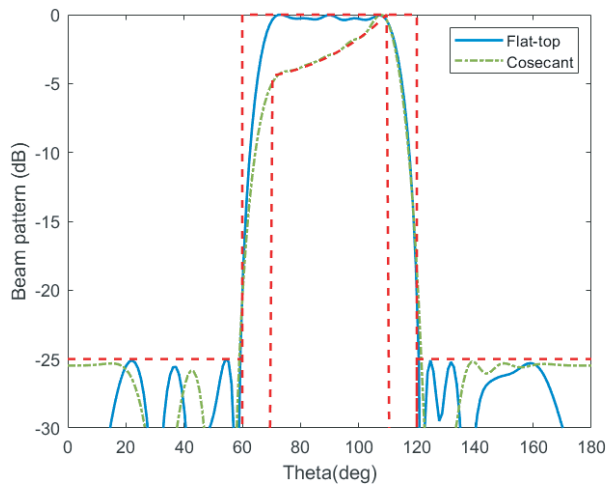


FIGURE 17. Synthesized cosecant and flat-top pattern.

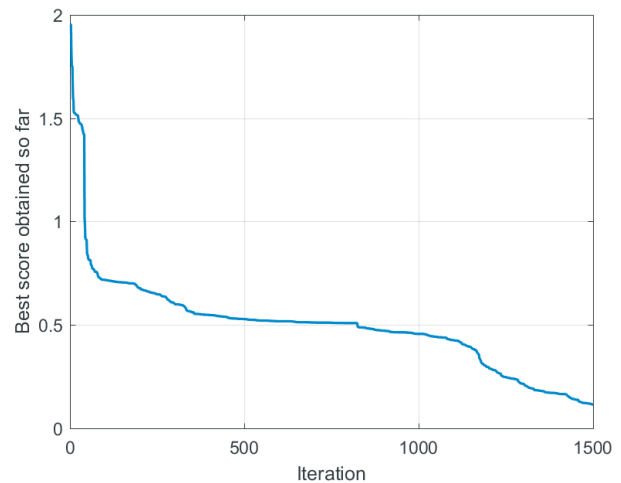


FIGURE 18. Synthesized cosecant and flat-top pattern.

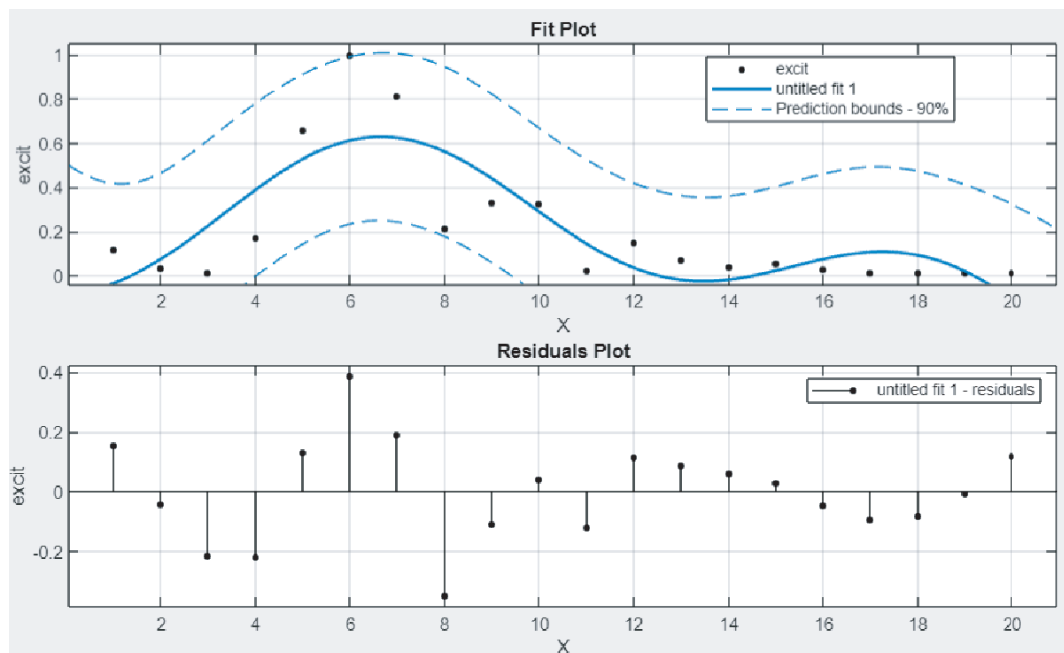


FIGURE 19. Common excitation amplitude of synthesized cosecant and flat-top pattern.

obtained by the proposed HWOA achieve the prescribed goals in this case. The directivities of the pencil beam and cosecant beam are 0.5464 and 0.3058, and DRR is 9.72.

6.2.4. Pencil Pattern vs Flat-Top vs Cosecant Pattern

Due to containing more constraints, three reconfigurable patterns synthesis becomes a more difficult problem than two reconfigurable patterns synthesis for the evolution algorithm.

Through the optimization, the synthesized patterns and convergence curve obtained by HWOA are depicted in Fig. 25 and Fig. 26, and the corresponding excitation amplitude and phase are shown in Fig. 27 and Fig. 28. The PSLLs of the synthesized pencil, flat-top, and cosecant pattern reach -27.57 dB, -25.07 dB, and -25.19 dB, respectively. The maximal rip-

ples of the synthesized flat-top and cosecant pattern are 0.4 dB and 0.7898 dB. As can be seen from Fig. 25, the metrics of the synthesized patterns all meet the prescribed requirements. The directivities of pencil, cosecant, and flat-top beam are 0.5464, 0.3058, and 0.2826, and DRR is 97.71.

6.3. Synthesis of Envelope Pattern in the Side Lobe Region

6.3.1. Slope Line Envelope

Consider a 40-element linear array with a uniform spacing of $\lambda/2$. The aim of this example is to achieve a line envelop in the region of side lobe of the pencil pattern, keeping the beam width of the synthesized pattern not to be increased at the same time. Herein, the excitation amplitude is regarded as the optimization

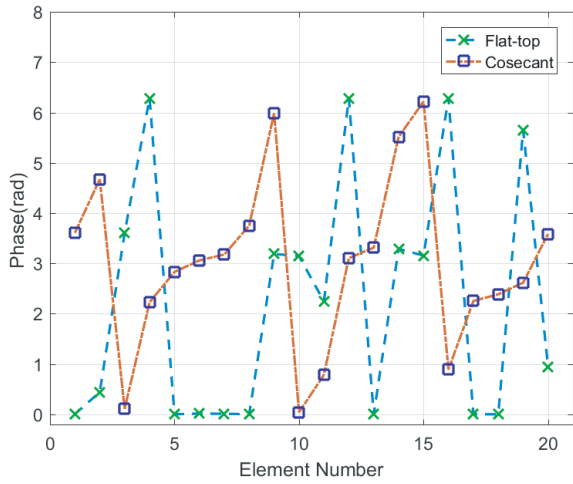


FIGURE 20. Excitation phase of synthesized cosecant and flat-top pattern.

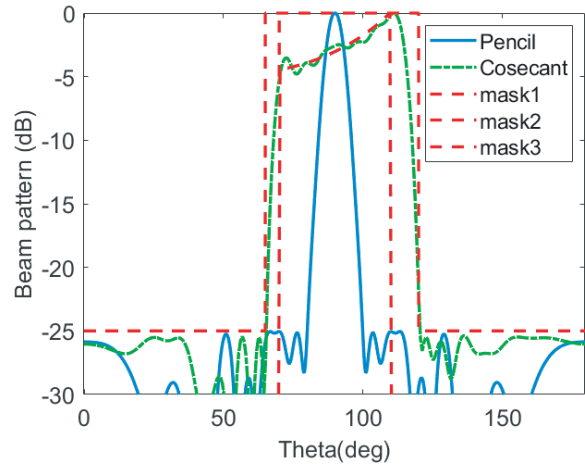


FIGURE 21. Synthesized pencil and cosecant pattern.

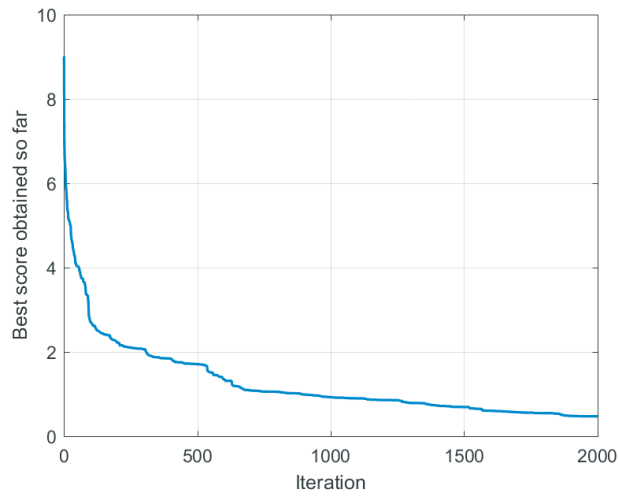


FIGURE 22. Convergence curve of synthesized pencil and cosecant pattern.

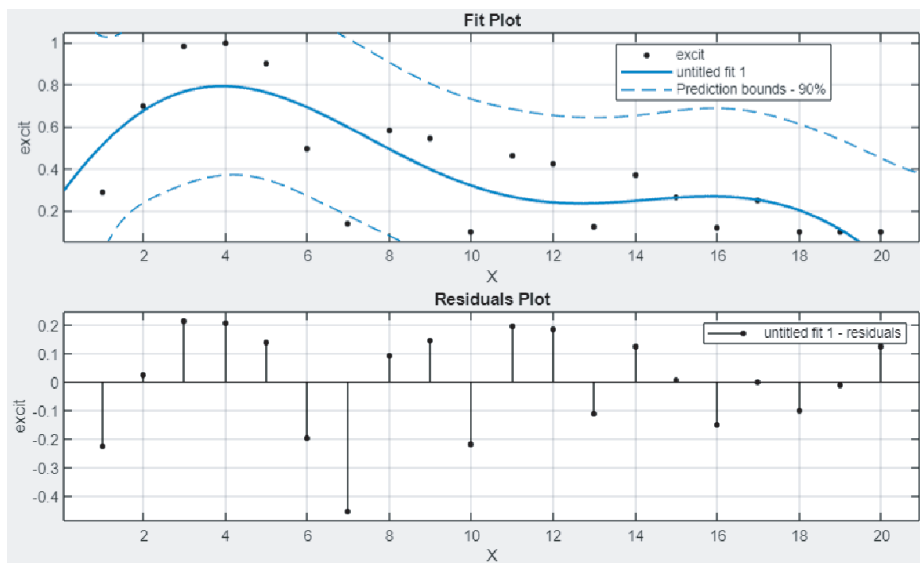


FIGURE 23. Excitation amplitude of synthesized pencil and cosecant pattern.

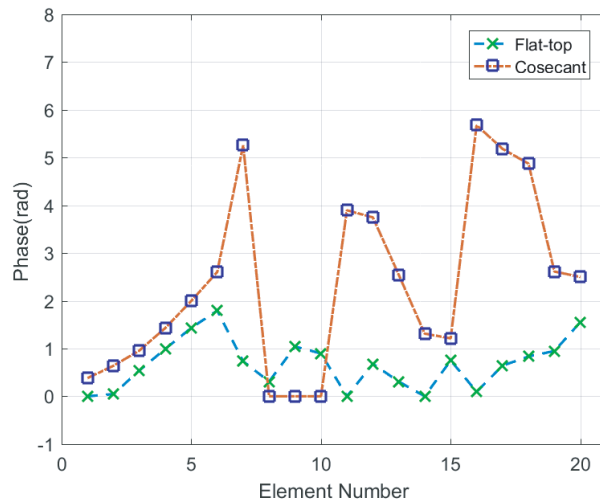


FIGURE 24. Excitation phase of synthesized pencil and cosecant pattern.

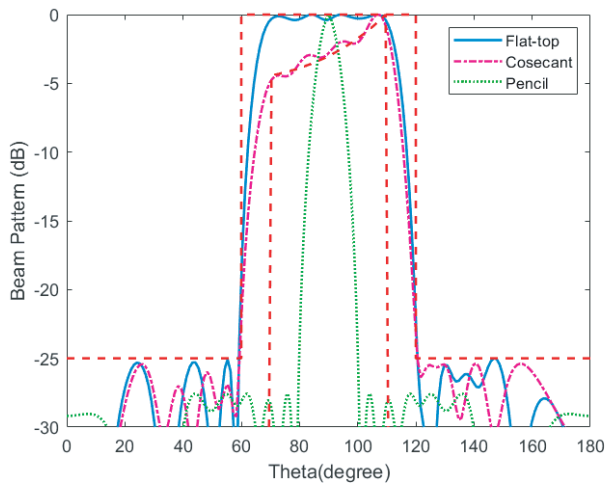


FIGURE 25. Synthesized multiple reconfigurable patterns.

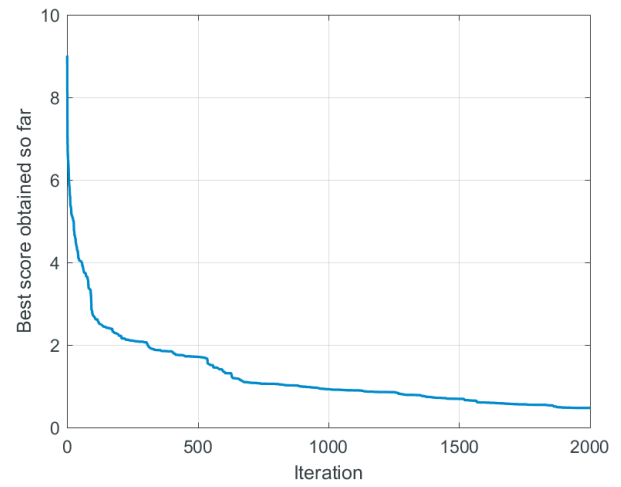


FIGURE 26. Convergence curve of synthesized multiple reconfigurable patterns.

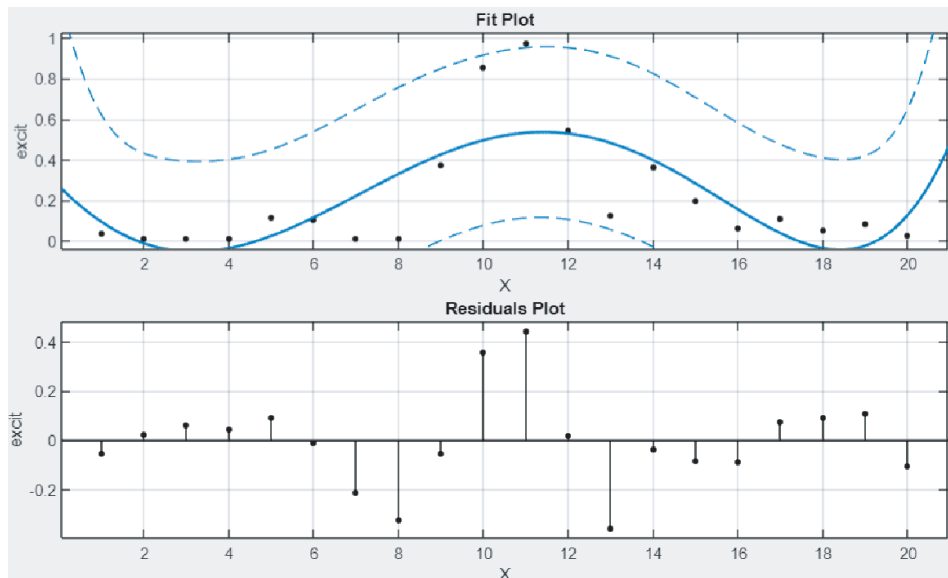


FIGURE 27. Common excitation amplitude of synthesized multiple reconfigurable patterns.

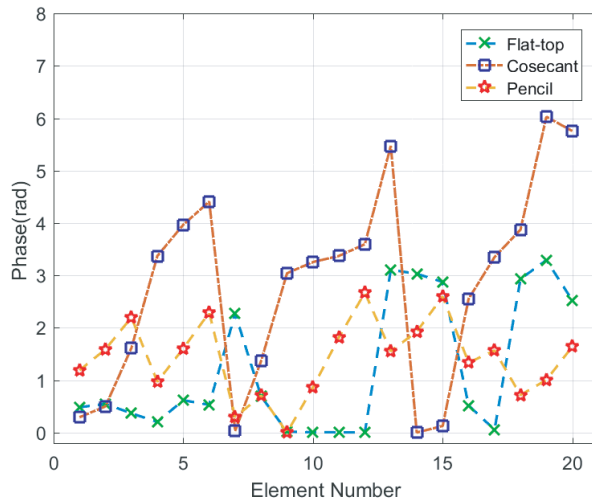


FIGURE 28. Excitation phase of synthesized three reconfigurable patterns.

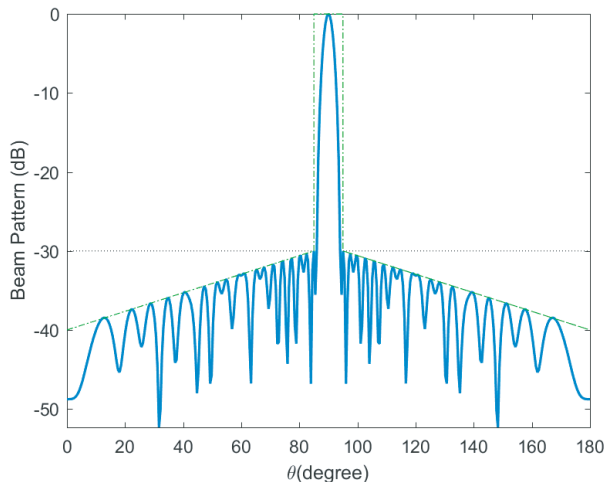


FIGURE 29. The obtained slope line envelope pattern.

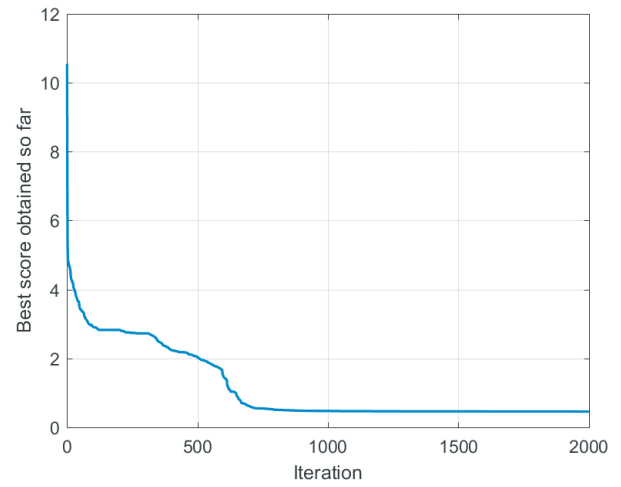


FIGURE 30. Convergence curve of slope line envelope synthesis.

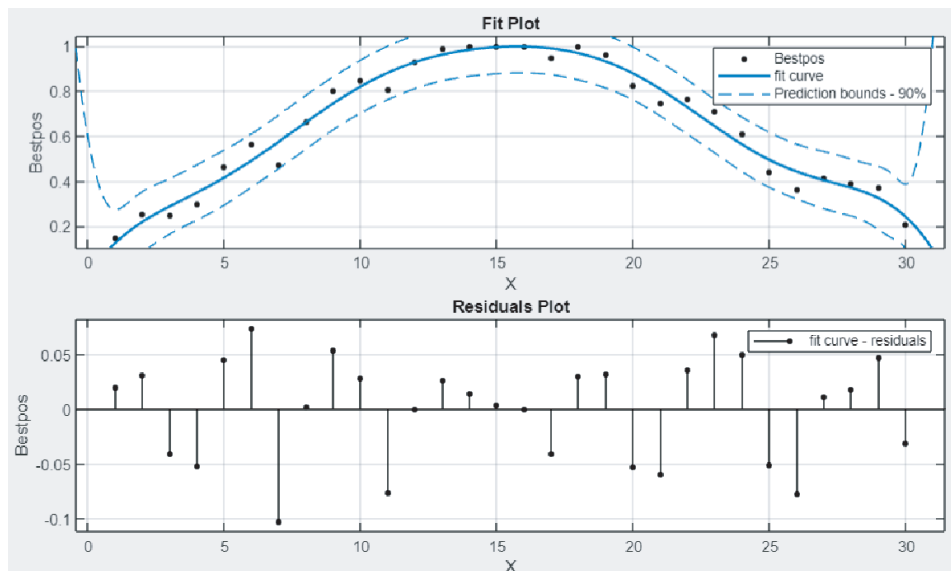


FIGURE 31. Excitation amplitude of slope line envelope.

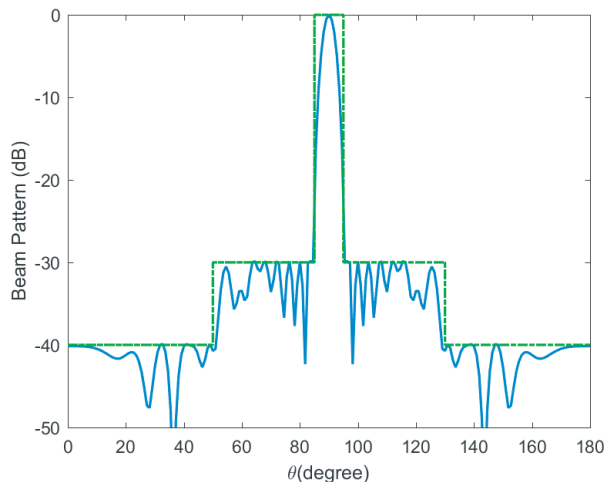


FIGURE 32. The obtained stair envelope pattern.

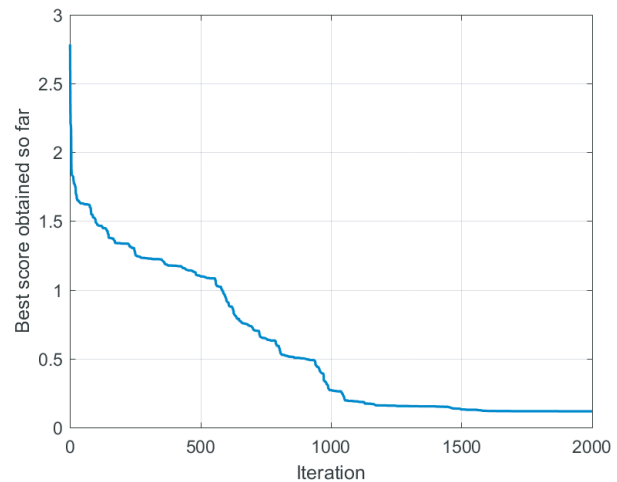


FIGURE 33. Convergence curve of stair envelope synthesis.

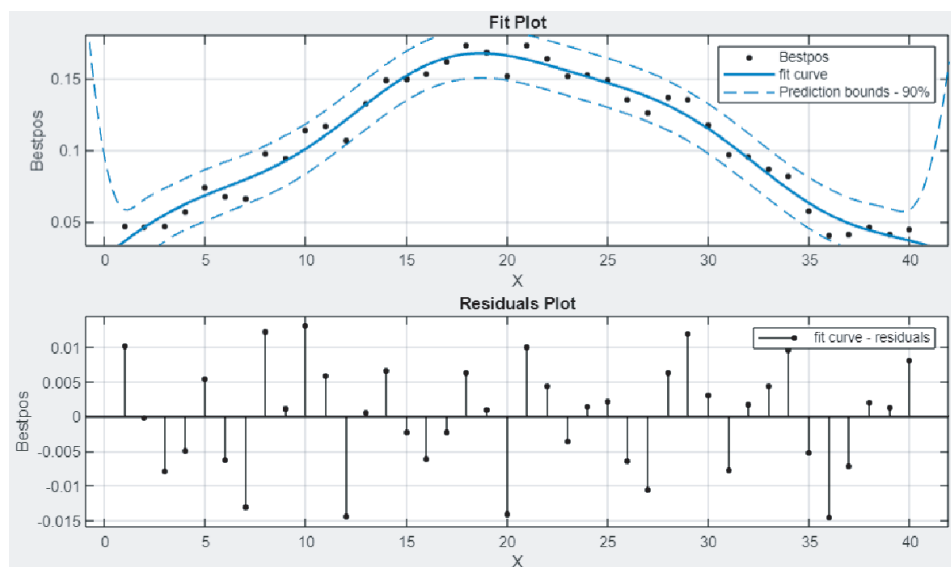


FIGURE 34. Excitation amplitude of stair envelope.

variable. The region of the main lobe lies in $\theta \in [85^\circ, 95^\circ]$. The side lobe levels are decreased from -30 dB to -40 dB along a line, below which all the side lobes lie. The maximal error between the synthesized beam and desired beam is 0.2 dB.

The synthesized pattern, convergence curve, and the corresponding excitation amplitude are shown in Fig. 29, Fig. 30, and Fig. 31. It can be seen that the synthesized envelop obtained by HWOA achieves the prescribed goal, and all the side lobe levels are located below the prescribed envelop. The directivity of beam is 1.6354 , and DRR is 4.28 .

6.3.2. Stair Envelope

In this example, we consider a 30-element linear array with an uniform spacing of $\lambda/2$. The aim of this case is to achieve a stair envelop over the side lobe region. The requirements of

the desired envelop are as follows: the main lobe region lies in $\theta \in [90^\circ \pm 5^\circ]$, and the expected PSLs in the side lobe region can be assigned as follows

$$\text{PSLL} = \begin{cases} -40 \text{ dB}, & \theta \in [0^\circ, 50^\circ] \\ -30 \text{ dB}, & \theta \in [50^\circ, 85^\circ] \end{cases} \quad (29)$$

The synthesized pattern, convergence curve, and the corresponding excitation amplitude are shown in Fig. 32, Fig. 33, and Fig. 34. The PSL of $\theta \in [0^\circ, 50^\circ]$ reaches -39.91 dB, which is close to the expected -40 dB. In the region of $\theta \in [50^\circ, 85^\circ]$, the synthesized pattern has a PSL of -29.87 dB. Fig. 32 shows that the PSLs of two regions do not reach a satisfactory expected level; however, the errors are marginal. For the shape of envelop, the optimal pattern obtained by HWOA achieves the requirements of the expected envelop. The directivity of beam is 2.1005 , and DRR is 6.77 .

7. CONCLUSION

In this paper, a new evolutionary technique called HWOA is proposed for synthesis of the problem of shaped, reconfigurable pattern and envelop. HWOA integrates IWO and Chen chaotic attractor into WOA, in order to improve the global search capability, achieve the faster convergence speed, high accuracy, and effectively get rid of a local optimum. The proposed HWOA has been evaluated by the classical benchmark functions. The test results of HWOA are compared with those of the state-of-the-art algorithms to demonstrate its superiority. The simulation result shows that the proposed HWOA can enhance the diversity of population against jumping out of the local optima and balance the exploitation and exploration capability, due to introducing the chaotic strategy and IWO.

HWOA is applied to the synthesis of the shaped, reconfigurable, and envelope beam. Examples are provided, and the numerical results are obtained. As can be seen, HWOA can achieve a satisfactory pattern, and meet the prescribed goals for the synthesis of shaped, reconfigurable and envelope beam.

In [47], the authors proposed a method to design a circularly polarized antenna for short-range communications. Since the selection of suitable parameters is an important problem in the design of antenna, HWOA can solve it. We hope that HWOA can be extended into various types of antenna array for short-range communications in the future. Additionally, it would be interesting to hybridize WOA with other evolutionary algorithms like wind driven optimization. Also, we will explore the use of WOA-based hybrid algorithm to solve the real world problem in the field of antenna array.

ACKNOWLEDGEMENT

This work was supported in part by Key Research Project of Gansu University of Political Science and Law (grant No. GZF2023XZD17), Soft Science Special Project of Gansu Basic Research Plan (grant No. 22JR11RA106), and Key Research Project of Gansu University of Political Science and Law (grant No. GZF2022XZD08).

REFERENCES

- [1] Schelkunoff, S. A., "A mathematical theory of linear arrays," *The Bell System Technical Journal*, Vol. 22, No. 1, 80–107, 1943.
- [2] Woodward, P. M., "A method of calculating the field over a plane aperture required to produce a given polar diagram," *Journal of the Institution of Electrical Engineers — Part IIIA: Radiolocation*, Vol. 93, No. 10, 1554–1558, 1946.
- [3] Orchard, H. J., R. S. Elliott, and G. J. Stern, "Optimising the synthesis of shaped beam antenna patterns," *IEE Proceedings H (Microwaves, Antennas and Propagation)*, Vol. 132, No. 1, 63–68, 1985.
- [4] Stutzman, W., "Synthesis of shaped-beam radiation patterns using the iterative sampling method," *IEEE Transactions on Antennas and Propagation*, Vol. 19, No. 1, 36–41, 1971.
- [5] Mautz, J. and R. Harrington, "Computational methods for antenna pattern synthesis," *IEEE Transactions on Antennas and Propagation*, Vol. 23, No. 4, 507–512, 1975.
- [6] Bucci, O. M., G. D'Elia, G. Mazzarella, and G. Panariello, "Antenna pattern synthesis: A new general approach," *Proceedings of the IEEE*, Vol. 82, No. 3, 358–371, 1994.
- [7] Ares, F., R. S. Elliott, and E. Moreno, "Design of planar arrays to obtain efficient footprint patterns with an arbitrary footprint boundary," *IEEE Transactions on Antennas and Propagation*, Vol. 42, No. 11, 1509–1514, 1994.
- [8] Bhattacharyya, A. K., "Projection matrix method for shaped beam synthesis in phased arrays and reflectors," *IEEE Transactions on Antennas and Propagation*, Vol. 55, No. 3, 675–683, 2007.
- [9] Ares-Pena, F. J., J. A. Rodriguez-Gonzalez, E. Villanueva-Lopez, and S. R. Rengarajan, "Genetic algorithms in the design and optimization of antenna array patterns," *IEEE Transactions on Antennas and Propagation*, Vol. 47, No. 3, 506–510, 1999.
- [10] Liao, W.-P. and F.-L. Chu, "Array pattern nulling by phase and position perturbations with the use of the genetic algorithm," *Microwave and Optical Technology Letters*, Vol. 15, No. 4, 251–256, 1997.
- [11] Haupt, R. L., "Phase-only adaptive nulling with a genetic algorithm," *IEEE Transactions on Antennas and Propagation*, Vol. 45, No. 6, 1009–1015, 1997.
- [12] Marciano, D. and F. Duran, "Synthesis of antenna arrays using genetic algorithms," *IEEE Antennas and Propagation Magazine*, Vol. 42, No. 3, 12–20, 2000.
- [13] Trucco, A., "Thinning and weighting of large planar arrays by simulated annealing," *IEEE Transactions on Ultrasonics, Ferroelectrics, and Frequency Control*, Vol. 46, No. 2, 347–355, 1999.
- [14] Rodriguez, J. A., F. Ares, and E. Moreno, "Linear array pattern synthesis optimizing array element excitations using the simulated annealing technique," *Microwave and Optical Technology Letters*, Vol. 23, No. 4, 224–226, 1999.
- [15] Diaz, X., J. A. Rodríguez, F. Ares, and E. Moreno, "Design of phase-differentiated multiple-pattern antenna arrays," *Microwave and Optical Technology Letters*, Vol. 26, No. 1, 52–53, 2000.
- [16] Ravelo, B., G. Fontgalland, H. S. Silva, J. Nebhen, W. Rahajandraibe, M. Guerin, G. Chan, and F. Wan, "Original application of stop-band negative group delay microwave passive circuit for two-step stair phase shifter designing," *IEEE Access*, Vol. 10, 1493–1508, 2021.
- [17] Ravelo, B., M. Guerin, J. Frnda, F. E. Sahoo, G. Fontgalland, H. S. Silva, S. Ngoho, F. Haddad, and W. Rahajandraibe, "Design method of constant phase-shifter microwave passive integrated circuit in 130-nm BiCMOS technology with bandpass-type negative group delay," *IEEE Access*, Vol. 10, 93 084–93 103, 2022.
- [18] Baskar, S., A. Alphones, and P. N. Suganthan, "Genetic-algorithm-based design of a reconfigurable antenna array with discrete phase shifters," *Microwave and Optical Technology Letters*, Vol. 45, No. 6, 461–465, 2005.
- [19] Mahanti, G., A. Chakraborty, and S. Das, "Phase-only and amplitude-phase only synthesis of dual-beam pattern linear antenna arrays using floating-point genetic algorithms," *Progress In Electromagnetics Research*, Vol. 68, 247–259, 2007.
- [20] Boeringer, D. W. and D. H. Werner, "Particle swarm optimization versus genetic algorithms for phased array synthesis," *IEEE Transactions on Antennas and Propagation*, Vol. 52, No. 3, 771–779, 2004.
- [21] Gies, D. and Y. Rahmat-Samii, "Particle swarm optimization for reconfigurable phase-differentiated array design," *Microwave and Optical Technology Letters*, Vol. 38, No. 3, 168–175, 2003.
- [22] Li, X. and M. Yin, "Hybrid differential evolution with biogeography-based optimization for design of a reconfigurable antenna array with discrete phase shifters," *International Journal*

- of *Antennas and Propagation*, Vol. 2011, 2011.
- [23] Li, X. and M. Yin, "Design of a reconfigurable antenna array with discrete phase shifters using differential evolution algorithm," *Progress In Electromagnetics Research B*, Vol. 31, 29–43, 2011.
- [24] Hansen, R. C., "Array pattern control and synthesis," *Proceedings of the IEEE*, Vol. 80, No. 1, 141–151, 1992.
- [25] Boeringer, D. W., D. H. Werner, and D. W. Machuga, "A simultaneous parameter adaptation scheme for genetic algorithms with application to phased array synthesis," *IEEE Transactions on Antennas and Propagation*, Vol. 53, No. 1, 356–371, 2005.
- [26] Li, W.-T., X.-W. Shi, and Y.-Q. Hei, "An improved particle swarm optimization algorithm for pattern synthesis of phased arrays," *Progress In Electromagnetics Research*, Vol. 82, 319–332, 2008.
- [27] Bera, R., S. Cheruvu, K. Kundu, P. Upadhyay, and D. Mandal, "Array antenna pattern synthesis using improved particle swarm optimization (IPSO) algorithm," *ECTI Transactions on Electrical Engineering, Electronics, and Communications*, Vol. 21, No. 2, 249 806–249 806, 2023.
- [28] Sun, Y., J. Sun, and L. Ye, "Synthesis of thinned planar concentric circular antenna arrays using a modified artificial bee colony algorithm," *International Journal of Antennas and Propagation*, Vol. 2023, No. 1, 7735267, 2023.
- [29] Yuan, P., C. Guo, J. Ding, and Y. Qu, "Synthesis of nonuniform sparse linear array antenna using whale optimization algorithm," in *2017 Sixth Asia-Pacific Conference on Antennas and Propagation (APCAP)*, 1–3, Xi'an, China, 2017.
- [30] Mirjalili, S. and A. Lewis, "The whale optimization algorithm," *Advances in Engineering Software*, Vol. 95, 51–67, 2016.
- [31] Bhesdadiya, R., P. Jangir, N. Jangir, I. N. Trivedi, and D. Ladumor, "Training multi-layer perceptron in neural network using whale optimization algorithm," *Indian Journal of Science & Technology*, Vol. 9, No. 19, 28–36, 2016.
- [32] Trivedi, I. N., J. Pradeep, J. Narottam, K. Arvind, and L. Dilip, "Novel adaptive whale optimization algorithm for global optimization," *Indian Journal of Science and Technology*, Vol. 9, No. 38, 1–6, 2016.
- [33] Aljarah, I., H. Faris, and S. Mirjalili, "Optimizing connection weights in neural networks using the whale optimization algorithm," *Soft Computing*, Vol. 22, 1–15, 2018.
- [34] Kaveh, A. and M. I. Ghazaan, "Enhanced whale optimization algorithm for sizing optimization of skeletal structures," *Mechanics Based Design of Structures and Machines*, Vol. 45, No. 3, 345–362, 2017.
- [35] Ling, Y., Y. Zhou, and Q. Luo, "Lévy flight trajectory-based whale optimization algorithm for global optimization," *IEEE Access*, Vol. 5, 6168–6186, 2017.
- [36] Mafarja, M. M. and S. Mirjalili, "Hybrid whale optimization algorithm with simulated annealing for feature selection," *Neuro-computing*, Vol. 260, 302–312, 2017.
- [37] Yuan, P., C. Guo, Q. Zheng, and J. Ding, "Sidelobe suppression with constraint for MIMO radar via chaotic whale optimisation," *Electronics Letters*, Vol. 54, No. 5, 311–313, 2018.
- [38] Yuan, P., C.-J. Guo, G. Jiang, and Q. Zheng, "Two-way pattern synthesis of MIMO radar with sidelobe reduction and null control via improved whale optimization algorithm," *Progress In Electromagnetics Research C*, Vol. 94, 45–57, 2019.
- [39] Yuan, P., C.-J. Guo, and Q. Zheng, "Synthesis of MIMO system with scattering using binary whale optimization algorithm with crossover operator," *Progress In Electromagnetics Research Letters*, Vol. 87, 21–28, 2019.
- [40] Patel, P., G. Kumari, and P. Saxena, "Array pattern correction in presence of antenna failures using metaheuristic optimization algorithms," in *2019 International Conference on Communication and Signal Processing (ICCSP)*, 0695–0700, Chennai, India, 2019.
- [41] Poddar, S., P. Paul, A. Chakraborty, G. Ram, and D. Mandal, "Design optimization of linear arrays and time-modulated antenna arrays using meta-heuristics approach," *International Journal of Numerical Modelling: Electronic Networks, Devices and Fields*, Vol. 35, No. 5, e3010, 2022.
- [42] Tang, B., L. Cai, S. Yang, J. Xu, and Y. Yu, "Evolutionary computation for sparse synthesis optimization of CCAAs: An enhanced whale optimization algorithm method," *Future Internet*, Vol. 14, No. 12, 347, 2022.
- [43] Prabhakar, D., K. Srinivas, R. Spandana, D. Anusha, M. Srikanth, and Y. R. Krishna, "The synthesis of elliptical antenna array using hybrid SSWOA algorithm," *Applied Computational Electromagnetics Society Journal*, Vol. 38, No. 5, 309, 2023.
- [44] Mehrabian, A. R. and C. Lucas, "A novel numerical optimization algorithm inspired from weed colonization," *Ecological Informatics*, Vol. 1, No. 4, 355–366, 2006.
- [45] Chen, G. and T. Ueta, "Yet another chaotic attractor," *International Journal of Bifurcation and Chaos*, Vol. 9, No. 07, 1465–1466, 1999.
- [46] Gao, S., Y. Yu, Y. Wang, J. Wang, J. Cheng, and M. Zhou, "Chaotic local search-based differential evolution algorithms for optimization," *IEEE Transactions on Systems, Man, and Cybernetics: Systems*, Vol. 51, No. 6, 3954–3967, 2019.
- [47] Leonardi, O., M. G. Pavone, G. Sorbello, A. F. Morabito, and T. Isernia, "Compact single-layer circularly polarized antenna for short-range communication systems," *Microwave and Optical Technology Letters*, Vol. 56, No. 8, 1843–1846, 2014.